

# Physics of suction cups in air and in water

A. Tiwari<sup>1</sup> and B.N.J. Persson<sup>1,2</sup>

<sup>1</sup>*PGI-1, FZ Jülich, Germany, EU*

<sup>2</sup>*www.MultiscaleConsulting.com*

We present experimental results for the dependency of the pull-off time (failure time) on the pull-off force for suction cups in the air and in water. The results are analyzed using a theory we have developed for the contact between suction cups and randomly rough surfaces. The theory predicts the dependency of the pull-off time (failure time) on the pull-off force, and is tested with measurements performed on suction cups made from a soft polyvinyl chloride (PVC). As substrates we used sandblasted poly(methyl methacrylate) (PMMA). The theory is in good agreement with the experiments in air, except for surfaces with the root-mean-square (rms) roughness below  $\approx 1 \mu\text{m}$ , where we observed lifetimes much longer than predicted by the theory. We show that this is due to out-diffusion of plasticizer from the soft PVC, which block the critical constrictions along the air flow channels. In water some deviation between theory and experiments is observed which may be due to capillary forces. We discuss the role of cavitation for the failure time of suction cups in water.

## 1 Introduction

All solids have surface roughness which has a huge influence on a large number of physical phenomena such as adhesion, friction, contact mechanics and the leakage of seals[1–13]. Thus when two solids with nominally flat surfaces are squeezed into contact, unless the applied squeezing pressure is high enough, or the elastic modulus of at least one of the solids low enough, a non-contact region will occur at the interface. If the non-contact region percolate there will be open channels extending from one side of the nominal contact region to the other side. This will allow fluid to flow at the interface from a high fluid pressure region to a low pressure region.

For elastic solids with randomly rough surfaces the contact area percolate when the relative contact area  $A/A_0 \approx 0.42$  (see [14]), where  $A_0$  is the nominal contact area and  $A$  the area of real contact (projected on the  $xy$ -plane). When the contact area percolate there is no open (non-contact) channel at the interface extending across the nominal contact region, and no fluid can flow between the two sides of the nominal contact.

The discussion above is fundamental for the leakage of static seals[15–18]. Here we are interested in rubber suction cups. In this application, the contact between the suction cup and the counter surface (which form an annulus) must be so tight that negligible fluid can flow from outside the suction cup to inside it.

Suction cups find ubiquitous usage in our everyday activities such as hanging of items to smooth surfaces in our houses and cars, and for technologically demanding applications such as lifting fragile and heavy objects safely in a controlled manner using suction cups employing vacuum pumps. Suction cups are increasingly used in robotic applications, such as robots which can climb walls and clean windows. The biomimetic design of suction cups based on octopus vulgaris, remora (sucker fish), limpets and Northern Clingfish is an area of current scientific investigations whose main objectives is to manufacture suc-

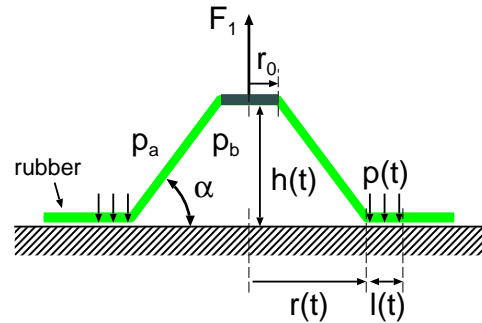


FIG. 1: Schematic picture of the suction cup pull-off experiment used in the present study. The container with the suction cup is either empty or filled with distilled water.

tion cups exhibiting adhesion under water and on surfaces with varying degree of surface roughness[19, 20]. Recently Iwasaki et. al. have presented the concept of magnet embedded suction cups for in-vivo medical applications[21].

## 2 Theory: gas leakage

The suction cups we study below can be approximated as a truncated cone with the diameter  $2r_1$ . The angle  $\alpha$  and the upper plate radius  $r_0$  are defined in Fig. 1. When a suction cup is pressed in contact with a flat surface the rubber cone will make apparent contact with the substrate in an annular region, but the contact pressure will be largest in a smaller annular region of width  $l(t)$  formed close to the inner edge of the nominal contact area (see Fig. 1). We will assume that the rubber-substrate contact pressure in this region of space is constant,  $p = p(t)$ , and zero elsewhere.

If we define  $h_0 = r_0 \tan \alpha$  the volume of gas inside the suction cup is

$$V = \pi r^2 \frac{1}{3} (h + h_0) - \pi r_0^2 \frac{1}{3} h_0$$

Since

$$\frac{r}{r_0} = 1 + \frac{h}{h_0} \quad (1)$$

we get

$$V = V_0 \left[ \left( \frac{r}{r_0} \right)^3 - 1 \right] \quad (2)$$

where  $V_0 = \pi r_0^2 h_0 / 3$ . The elastic deformation of the rubber film (cone) needed to make contact with the substrate require a normal force  $F_0(h)$ , which we will refer to as the cup (non-linear) spring-force. This force result from the bending of the film and to the (in-plane) stretching and compression of the film needed to deform (part of) the conical surface into a flat circular disc or annulus. The function  $F_0(h)$  can be easily measured experimentally (see below).

We assume that the rubber cup is in repulsive contact with the substrate over a region of width  $l(t)$ . Since the thickness of the suction cup material decreases as  $r$  increases, we expect that  $l$  decreases as  $r$  increases. From optical pictures of the contact we have found that to a good approximation

$$l \approx l_0 + l_a \left( 1 - \frac{r}{r_0} \right) = l_0 - l_a \frac{h}{h_0} \quad (3)$$

where  $l_a = (l_1 - l_0) / (1 - r_1 / r_0)$  where  $l_1$  is the width of the contact region when  $r = r_1$ , and  $l_0$  the width of the contact region when  $r = r_0$ . The contact pressure  $p = p(t)$  in the circular contact strip is assumed to be constant

$$p \approx \frac{F_0(h)}{2\pi r l} + \beta(p_a - p_b) \quad (4)$$

where  $\beta$  is a number between 0 and 1, which takes into account that the gas pressure (in the non-contact region) in the strip  $l(t)$  changes from  $p_a$  for  $r > r(t) + l(t)$  to  $p_b$  for  $r < r(t)$ , while the outside pressure is  $p_a$ .

Assume that the pull-force  $F_1$  act on the suction cup (see Fig. 1). The sum of  $F_1$  and the cup spring-force  $F_0$  must equal the force resulting from the pressure difference between outside and inside the suction cup, i.e.

$$F_0 + F_1 = \pi r^2 (p_a - p_b) \quad (5)$$

We assume that the air can be treated as an ideal gas so that

$$p_b V_b = N_b k_B T. \quad (6)$$

The number of molecules per unit time entering the suction cup,  $\dot{N}_b(t)$ , is given by

$$\dot{N}_b = f(p, p_a, p_b) \frac{L_y}{L_x} \quad (7)$$

Here  $L_x$  and  $L_y$  are the lengths of the sealing region along and orthogonal to the gas leakage direction, respectively. In the present case

$$\frac{L_y}{L_x} = \frac{2\pi r}{l}$$

The (square-unit) leak-rate function  $f(p, p_a, p_b)$  will be discussed below.

The equations (1)-(7) constitute 7 equations from which the following 7 quantities can be obtained:  $h(t)$ ,  $r(t)$ ,  $l(t)$ ,  $V(t)$ ,  $p_b(t)$ ,  $p(t)$  and  $N_b(t)$ . The equations (1)-(7) can be easily solved by numerical integration.

The suction cup stiffness force  $F_0(h)$  depends on the speed with which the suction cup is compressed (or decompressed). The reason for this is the viscoelastic nature of the suction cup material. To take this effect into account we define the contact time state variable  $\phi(t)$  as [1, 22, 23]:

$$\dot{\phi} = 1 - \dot{r}\phi/l \quad (8)$$

with  $\phi(0) = 0$ . For stationary contact,  $\dot{r} = 0$ , this equation gives just the time  $t$  of stationary contact,  $\phi(t) = t$ . When the ratio  $\dot{r}/l$  is non-zero but constant (8) gives

$$\phi(t) = (1 - e^{-t/\tau}) \tau,$$

where  $\tau = l/\dot{r}$ . Thus for  $t \gg \tau$  we get  $\phi(t) = \phi_0 = \tau$ , which is the time a particular point on the suction cup surface stay in the rubber-substrate contact region of width  $l(t)$ . It is only in this part of the rubber-substrate nominal contact region where a strong (repulsive) interaction occur between the rubber film and the substrate, and it is region of space which is most important for the gas sealing process.

From dimensional arguments we expect that  $F_0(h)$  is proportional to the effective elastic modulus of the cup material. We have measured  $F_0(h)$  at a constant indentation speed  $\dot{h}$ , corresponding to a constant radial velocity  $\dot{r} = \dot{h}(r_0/h_0)$  (see (1)). In this case the effective elastic modulus is determined by the relaxation modulus  $E_{\text{eff}}(t)$  calculated for the contact time  $\phi_0 = l/\dot{r}$ . However, in general  $\dot{r}$  may be strongly time-dependent. We can take that into account by replacing the measured  $F_0(h)$  by the function  $F_0(h)E_{\text{eff}}(\phi(t))/E_{\text{eff}}(\phi_0)$ .

### 2.1 Diffusive and ballistic gas leakage

The gas leakage result from the open (non-contact) channels at the interface between the rubber film and the substrate. Most of the leakage occur in the biggest open flow channels. The most narrow constriction in the biggest open channels are denoted as the critical constrictions. Most of the gas pressure drop occur over the critical constrictions, which therefore determine the leak-rate to a good approximation. The surface separation in the critical constrictions is denoted by  $u_c$ . Theory shows that the lateral size of the critical constrictions is much

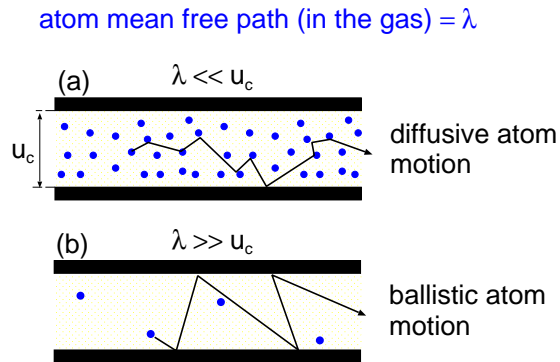


FIG. 2: Diffusive (a) and ballistic (b) motion of the gas atoms in the critical junction. In case (a) the gas mean free path  $\lambda$  is much smaller than the gap width  $u_c$  and the gas molecules makes many collisions with other gas molecules before a collision with the solid walls. In the opposite limit, when  $\lambda \gg u_c$  the gas molecules makes many collisions with the solid wall before colliding with another gas molecule. In the first case (a) the gas can be treated as a (compressible) fluid, but this is not the case in (b).

larger than the surface separation  $u_c$  (typically by a factor of  $\sim 100$ )[15–17].

In the theory for suction cups enters the leak-rate function  $f(p, p_a, p_b)$  (see (7)). This function can be easily calculated when the gas flow through the critical constrictions occur in the diffusive and ballistic limits (see Fig. 2). Here we present an interpolation formula which is (approximately) valid independent of the ratio between the gas mean free path and the surface separation at the critical constrictions:

$$\dot{N}_b = \frac{1}{24} \frac{L_y}{L_x} \frac{(p_a^2 - p_b^2)}{k_B T} \frac{u_c^3}{\eta} \left( 1 + 12 \frac{\eta \bar{v}}{(p_a + p_b) u_c} \right) \quad (9)$$

Here  $\eta$  is the gas viscosity and  $k_B T$  the thermal energy. The gas leakage equation (9) is in good agreement with treatment using the Boltzmann equation, and with experiments[24, 25]. To calculate  $u_c$  we need the relation between the interfacial separation  $u$  and the contact pressure  $p$ . For this we have used the Persson contact mechanics theory[13, 26, 27].

### 3 Experimental

We carried out the leakage experiments in air and water using two suction cups, denoted A and B, made from soft PVC. These suction cups have different geometrical designs, which has a influence on the suction cup stiffness and failure time, as discussed in section 3.2 and 4.1 respectively.

#### 3.1 Viscoelastic modulus of PVC

Viscoelastic modulus measurements of the suction cups A and B where carried out in oscillatory tension mode using a Q800 DMA instrument produced by TA Instruments. Fig. 3 shows (a) the temperature dependency of the low strain ( $\epsilon = 0.0004$ ) modulus  $E$ , and (b)

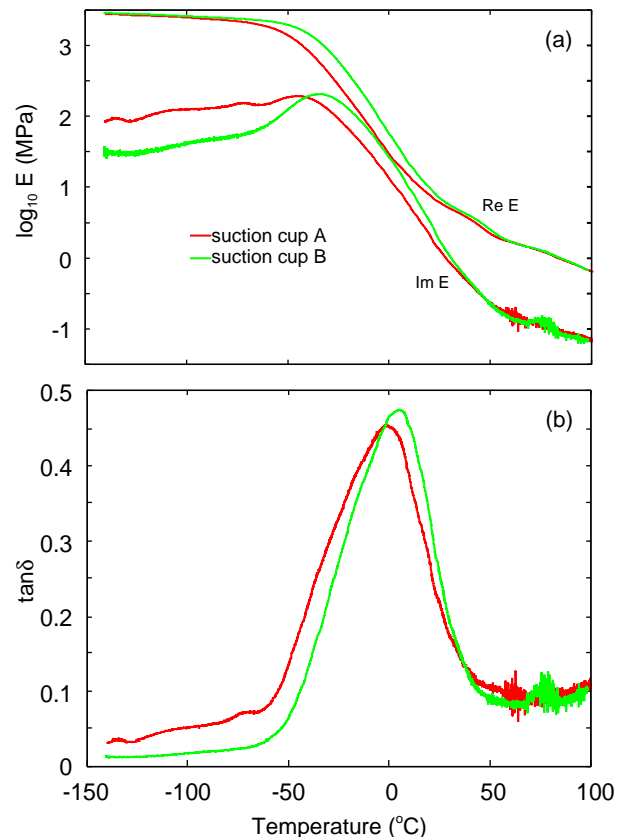


FIG. 3: The dependency of the low strain ( $\epsilon = 0.0004$ ) viscoelastic modulus (a), and  $\tan \delta = \text{Im}E/\text{Re}E$  (b), on the temperature for the frequency  $f = 1$  Hz. For the soft PVC of suction cup A (red) and B (green).

$\tan \delta = \text{Im}E/\text{Re}E$ , for the frequency  $f = 1$  Hz. Results are shown for the soft PVC of suction cup A (red lines) and B (green lines). Note that both materials exhibit very similar viscoelastic modulus. If we define the glass transition temperature as the temperature where  $\tan \delta$  is maximal (for the frequency  $f = 1$  Hz) then  $T_g \approx 0^\circ\text{C}$ .

#### 3.2 Suction cup stiffness force $F_0$

We have measured the relation between the normal force  $F_0$  and the normal displacement of the top of a suction cup. In the experiments we increase the displacement of the top plate (see Fig. 1) at a constant speed and measure the resulting force. We show results for two different suction cups, denoted A and B.

We have measured the force  $F_0$  for the suction cups squeezed against a smooth glass plate lubricated by soap water. The glass plate has a hole below the top of the suction cup; this allowed the air to leave the suction cup without any change in the pressure inside the suction cup (i.e.  $p_b = p_a$  is equal to the atmospheric pressure). Fig. 4 shows the stiffness force  $F_0(h)$  (in N) as a function of the squeezing (or compression) distance (in mm) for the suction cups A (red) and B (blue).

The suction cups A and B are both made from similar

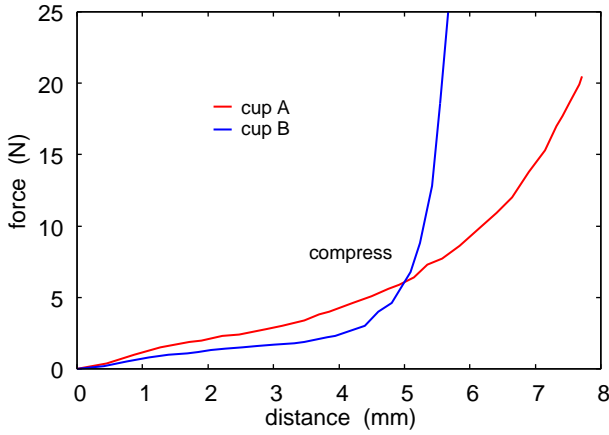


FIG. 4: The stiffness force  $F_0(h)$  (in N) as a function of the squeezing (or compression) distance (in mm) for the suction cups A (red) and B (blue). The suction cups are squeezed against a smooth glass plate with a hole in the center through which the air can leave so the air pressure inside the rubber suction cup is the same as outside (atmospheric pressure). The glass plate is lubricated with soap-water.

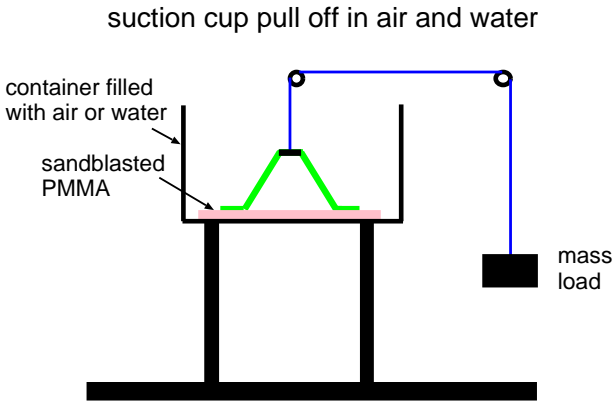


FIG. 5: Schematic picture of the experimental set-up for measuring the pull-off force in the air and in water.

type of soft PVC and both have the diameter  $\approx 4$  cm. However, for suction cup B the angle  $\alpha = 21^\circ$  in contrast to  $\alpha = 33^\circ$  for suction cup A, and the PVC film is thicker for the cup A. This difference in the angle  $\alpha$  and the film thickness influence the suction cup stiffness force as shown in Fig. 4. Note that before the strong increase in the  $F_0(h)$  curve which result when the suction cup is squeezed into complete contact with the counter surface the suction cup A has a stiffness nearly twice as high as that of the suction cup B.

#### 4 Experiment: Failure of suction cup in air

We have studied how the failure time of a suction cup depends on the pull-off force (vertical load) and the substrate surface roughness (see Fig. 5). The suction cup was always attached to the lower side of a horizontal surface and a mass-load was attached to the suction cup.

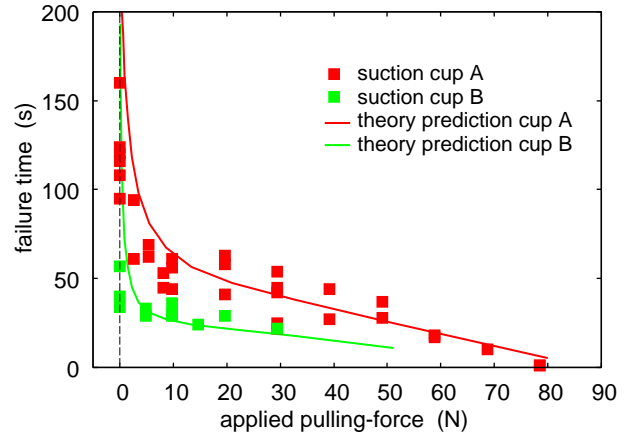


FIG. 6: The dependency of the pull-off time (failure time) on the applied (pulling) force. The soft PVC suction cups A and B are in contact with a sandblasted PMMA surface with the rms roughness  $1.89 \mu\text{m}$ . All surfaces were cleaned with soap water before the experiments.

We varied the mass-load from 0.25 kg to 8 kg. If full vacuum would prevail inside the suction cup, the maximum possible pull-off force would be  $\pi r_1^2 p_a$ . Using  $r_1 = 19$  mm and  $p_a = 100$  kPa we get  $F_{\text{max}} = 113$  N or about 11 kg mass load. However, the maximum load possible in our experiments for a smooth substrate surface is about 9 kg, indicating that no complete vacuum was obtained. This may, in least in part, be due to problems to fully remove the air inside the suction cup in the initial state. In addition we have found that for mass loads above 8 kg the pull-off is very sensitive to instabilities in the macroscopic deformations of the suction cup, probably resulting from small deviations away from the vertical direction of the applied loading force.

#### 4.1 The dependency of the failure time on the pull-off force

Fig. 6 shows the dependency of the pull-off time (failure time) on the applied pulling force. The results are for the soft PVC suction cups A (red) and B (green) in contact with a sandblasted PMMA surface with the rms-roughness  $1.89 \mu\text{m}$ . Before the measurement, all surfaces were cleaned with soap water. The solid lines are the theory predictions, using as input the surface roughness power spectrum of the PMMA surface, and the measured stiffness of the suction cup, the latter corrected for viscoelastic time-relaxation as described above. Note the good agreement between the theory and the experiments in spite of the simple nature of the theory.

Fig. 7(a) shows the calculated time dependency of the radius of the non-contact region, and (b) the gas pressure in the suction cup. We show results for several pull-off forces from  $F_1 = 5$  N in steps of 5 N to 80 N.

The smaller angle  $\alpha$  for suction cup B than for cup A imply that if the same amount of gas would leak into the suction cups the gas pressure  $p_b$  inside the suction

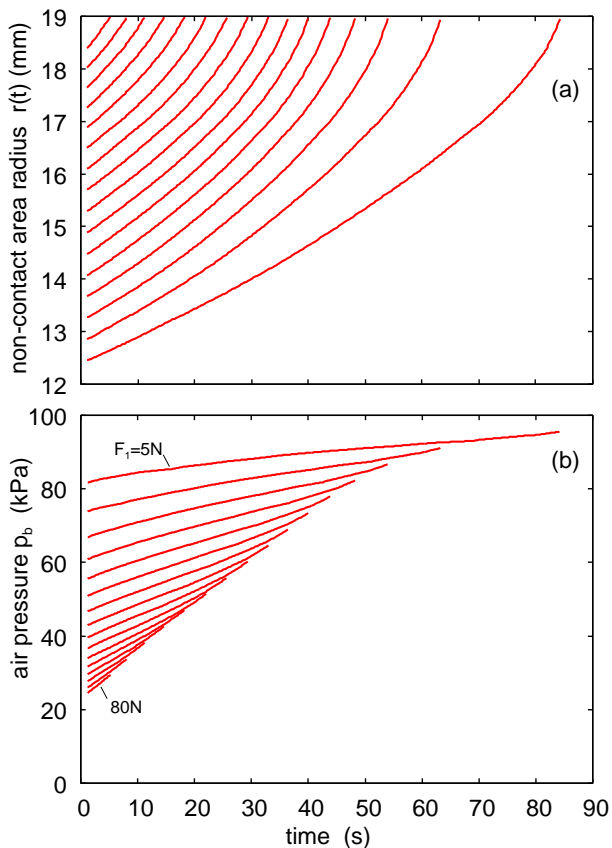


FIG. 7: The calculated dependency time dependency of the (a) radius of the non-contact region and (b) the pressure in the suction cup, for several pull-off forces (from  $F_1 = 5$  N in steps of 5 N to 80 N). The soft PVC suction cup is in contact with a sandblasted PMMA surface with the rms roughness  $1.89 \mu\text{m}$ .

cup will be highest for the suction cup B. This will tend to reduce the lifetime of cup B. Similarly, the smaller stiffness of the cup B result in smaller contact pressure  $p$ , which will increase the leakage rate and reduce the lifetime. Hence both effects will make the lifetime of the suction cup B smaller than that of the cup A.

#### 4.2 The dependency of the failure time on the surface roughness

Fig. 8 shows the dependency of the pull-off time (failure time) on the substrate surface roughness. The results are for the type A soft PVC suction cups in contact with sandblasted PMMA surfaces with different rms roughness, and a table surface. Note that for “large” roughness the predicted failure time is in good agreement with the measured data, but for rms roughness below  $\approx 1 \mu\text{m}$  the measured failure times are much larger than the theory prediction. In addition, the dependency of the radius  $r(t)$  of the non-contact region on time is very different in the two cases: For roughness larger than  $\approx 1 \mu\text{m}$  the radius increases continuously with time as also expected from theory (see Fig. 7(a)). For rough-

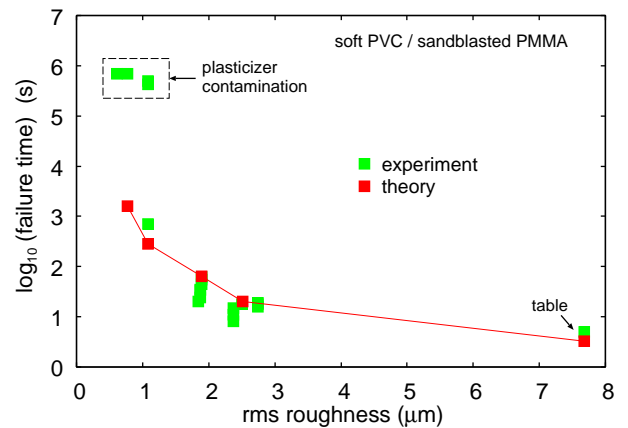


FIG. 8: The dependency of the pull-off time (failure time) on the substrate surface roughness. For soft PVC suction cups in contact with sandblasted PMMA surfaces with different rms-roughness, and a table surface. The pull-off force  $F_1 = 10$  N. All surfaces were cleaned with soap water before the experiments, and a new suction cup was used for each experiment.

ness below  $\approx 1 \mu\text{m}$  the boundary line  $r(t)$  stopped to move a short time after applying the pull-off force, and remained fixed until the detachment occurred by a rapid increase in  $r(t)$  (catastrophic event). We attribute this discrepancy between theory and experiments to transfer of plasticizer from the soft PVC to the PVC-PMMA interface; this (high viscosity) fluid will fill-up the critical constrictions and hence stop, or strongly reduce, the flow of air into the suction cup. This is consistent with many studies[28] of the transfer of plasticizer from soft PVC to various contacting materials. These studies show typical transfer rates (at room temperature) corresponding to a  $\sim 1-10 \mu\text{m}$  thick film of plasticizer after one week waiting time. Optical pictures of the rough PMMA surface after long contact with the suction cup A also showed darkened (and sticky) annular regions indicating transfer of material from the PVC to the PMMA surface.

#### 5 Theory: liquid (water) leakage

Assuming that the water can be treated as an incompressible Newtonian liquid, and assuming laminar flow, the volume of liquid flowing per unit time into the suction cup is given by

$$\dot{V}_b = \frac{1}{12\eta} \frac{L_y}{L_x} u_c^3 (p_a - p_b). \quad (10)$$

This equation replaces (9), which is valid for gas flow, but all the other equations are unchanged.

In the experiments reported on below, the suction cup is squeezed vertically into contact with the counter surface (here a PMMA sheet). Even if no gas (air) can be detected inside the suction cup before squeezing it in contact with the PMMA surface, after removing the squeezing force we always observe a gas filled region at the top of the suction cup (see Fig. 9). We believe this result from



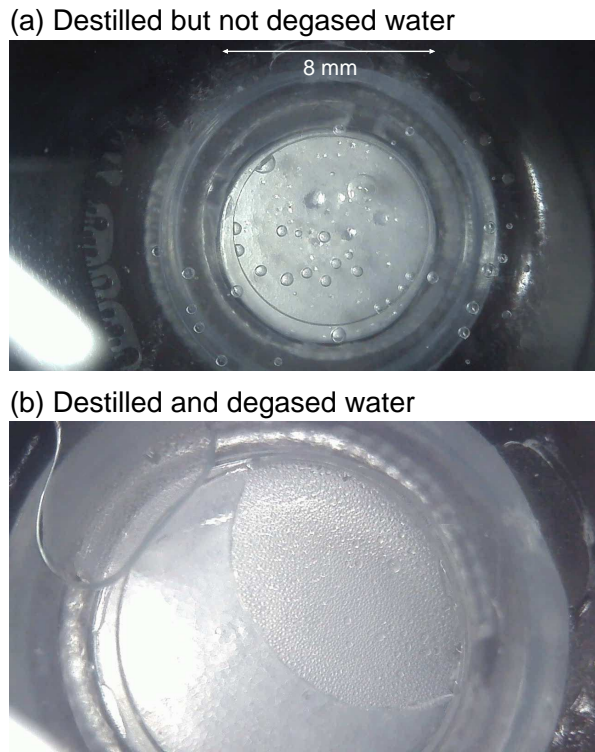


FIG. 9: Optical pictures of the center region of a suction cup after squeezing it against a smooth glass plate in (a) distilled but not degassed water, and (b) distilled and degassed (at 0.2 atmosphere pressure) water. In (a) we squeezed the cup with about 15 N against the glass plate, and then pulled it with a similar force for 10 s and then removed the pulling force and waited  $\sim 5$  minutes before taking the picture shown. In (b) we did the same but using a bigger squeezing and pulling force, about 60 N. In both cases cavitation has occurred, and we observed a slow evolution in time of the gas covered region. The central (or top) part of the suction cup is a flat circular metal disc (diameter 8 mm) covered by a PVC film. The magnification in (b) is higher than in (a). Note the condensation of small water droplets on the glass surface in the cavity region in (b). These droplets were growing with increasing time while the size of the gas bubble decreased slowly.

the spring force generating a reduced pressure inside the suction cup, which result in cavitation. When loaded with a pull-off force this gas region expand and result in a pressure inside the suction cup which is somewhere between atmospheric pressure and perfect vacuum (zero pressure). If all the air would have been removed, the pressure in the water could, at least initially, be negative (below vacuum), where the liquid is under mechanical tension. In fact, pressures as low as  $p_b \approx -20$  MPa has been observed for water at short times[29]. However, this state is only metastable and after long enough time one would expect the nucleation of a gas bubble in the liquid, and the liquid pressure would increase above zero. In fact, water in thermal (or kinetic) equilibrium with the normal atmosphere will have dissolved air molecules

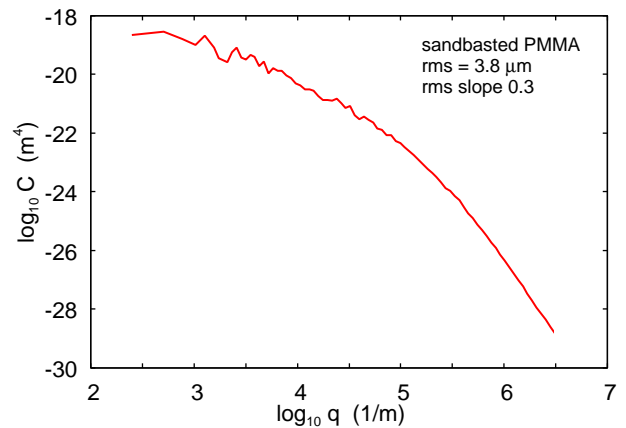


FIG. 10: The surface roughness power spectrum of sandblasted PMMA. Sandblasting was carried out for 10 min at a pressure of 8 bars. The root mean square roughness is  $3.8 \mu\text{m}$ .

(the volume ratio of dissolved gas (at atmospheric pressure) to water is about 0.04 at room temperature), and is unstable against cavitation whenever the pressure falls below the atmospheric pressure. Thus, the problem of determining the pressure in the fluid occurring inside the suction cup is nontrivial, and depend on trapped air bubbles and on how long time the reduced (compared to the atmospheric pressure) pressure prevail.

When a suction cup is used in water, when the pull-off force  $F_1 \rightarrow 0$ , at pull-off the suction cup contains water of atmospheric pressure. When a suction cup is used in the normal atmosphere the suction cup is instead filled with air of atmospheric pressure. Assuming an ideal gas the volume of air of atmospheric pressure flowing per unit time into the suction cup is determined by  $p_a \dot{V} = N_b k_B T$ . Using (9) this gives

$$\begin{aligned} \dot{V} &= \frac{1}{24} \frac{L_y}{L_x} \frac{(p_a^2 - p_b^2)}{p_a} \frac{u_c^3}{\eta} \left( 1 + 12 \frac{\eta \bar{v}}{(p_a + p_b) u_c} \right) \\ &= \frac{1}{12\eta} \frac{L_y}{L_x} u_c^3 (p_a - p_b) Q \end{aligned} \quad (11)$$

where

$$Q = \frac{p_a + p_b}{2p_a} \left( 1 + 12 \frac{\eta \bar{v}}{(p_a + p_b) u_c} \right) \quad (12)$$

Thus the gas leakage rate differ from the liquid leak-rate by a factor  $Q$ , which is a product of a factor  $(p_a + p_b)/2p_a$ , derived from the fact that the gas is a compressible fluid, and another factor arising from ballistic air flow. The latter factor does not exist in the liquid case because of the short molecule mean free path in the liquid.

## 6 Experiment: Failure of suction cup in water

We have studied the failure time for suction cup A immersed in distilled water. The experimental set up

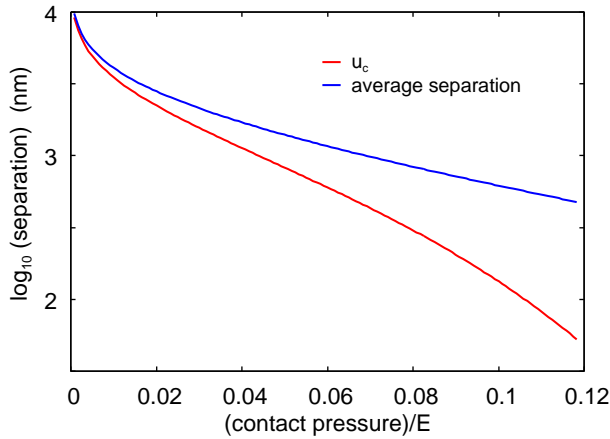


FIG. 11: The average surface separation  $\bar{u}$ , and the separation  $u_c$  at the critical constriction, as a function of the nominal contact pressure in units of the modulus  $E$ . For the surface with the power spectrum given in Fig. 10.

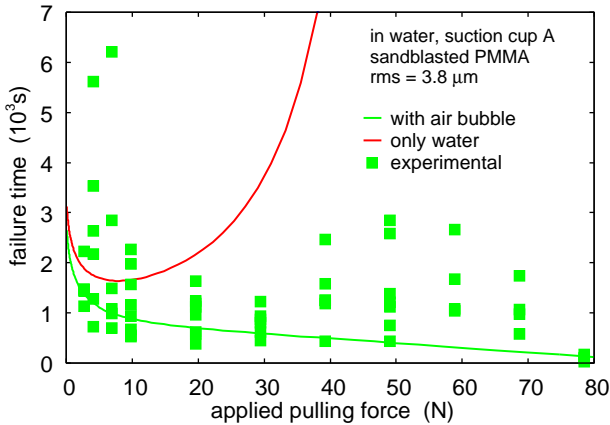


FIG. 12: Squares: The dependency of the failure time (time to pull-off) on the applied (pulling) force for the (soft PVC) suction cup in contact with a sandblasted PMMA surface (with the rms roughness  $3.8 \mu\text{m}$ ) in water. The red and green solid lines are the theory predictions assuming that in the initial state, before applying the pull-off force, there is some trapped water (but no air), or trapped air (but no water) inside the suction cup, so the initial radius of the detached region for no external load is about 10 mm. When only water occur, if the applied pull-force is big enough, a negative pressure (mechanical tension) develop in the water which will pull the surfaces further together in the contact strip  $l(t)$ . This reduces the water leakage and increases the failure time. When air occur in the suction cup the pressure is always positive, but below the atmospheric pressure.

is shown in Fig. 5. Here, the suction cup is squeezed against the rough PMMA countersurface under water. The water level is at least 20cm above the contacting interface. Fig. 10 shows the surface roughness power spectrum of the sandblasted PMMA surface used in water. The surface has the rms roughness amplitude  $3.8 \mu\text{m}$  and the rms slope 0.3.

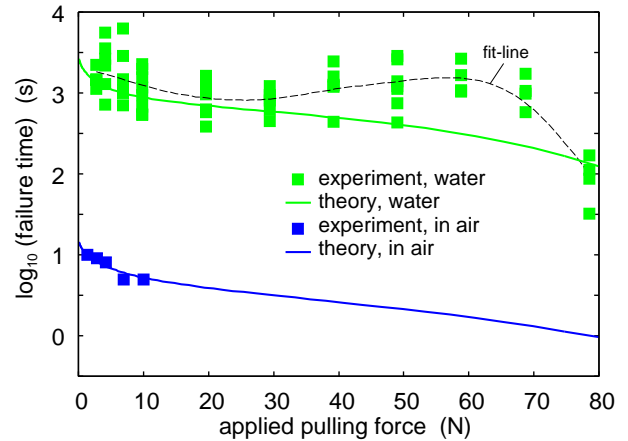


FIG. 13: Squares: The dependency of the logarithm of the failure time (time to pull-off) on the applied (pulling) force for the (soft PVC) suction cup in contact with a sandblasted PMMA surface (with the rms roughness  $3.8 \mu\text{m}$ ) in water (green) and in the air (blue). The green and blue solid lines are the theory predictions assuming that in the initial state, before applying the pull-off force, there is trapped air inside the suction cup, giving an initial radius of the detached region for no external load of  $\approx 10 \text{ mm}$  as observed experimentally. The black dashed line is a fit-line to the experimental data in water.

Using the power spectrum in Fig. 10 and the Persson contact mechanics theory, in Fig. 11 we show the calculated average surface separation  $\bar{u}$ , and the separation  $u_c$  at the critical constriction, as a function of the nominal contact pressure in units of the modulus  $E$  (with the Poisson ratio  $\nu = 0.5$ ). The Young's modulus of the suction cup (soft PVC) is of order (depending on the relaxation time) 2 – 4 MPa, and since the contact pressure is of order  $\approx 0.1 \text{ MPa}$ , we are interested in  $p/E$  below 0.1 and the separation at the critical constriction in most cases is of order a few  $\mu\text{m}$ .

At the start of a pull-off experiment the suction cup was squeezed against the PMMA surface with maximum possible hand-force (about 100 N). The squares in Fig. 12 shows the dependency of the failure time (time to pull-off) in water on the applied (pulling) force. It is remarkable that, on the average, the failure time increases with increasing pull-off force for  $F_1$  between  $\approx 30 \text{ N}$  and  $\approx 60 \text{ N}$  (see also dashed line in Fig. 13).

The solid lines in Fig. 12 are the theory predictions assuming that in the initial state, before applying the pull-off force, there is only trapped water (but no air) (red line), or trapped air (water with an air bubble) (green line) inside the suction cup. When only water occur, if the applied pull-force is big enough, a negative pressure (mechanical tension) develop in the water which will pull the surfaces further together in the contact strip of width  $l(t)$  (see last term in (4)). This reduces the water leakage and increases the failure time. When air occur in the

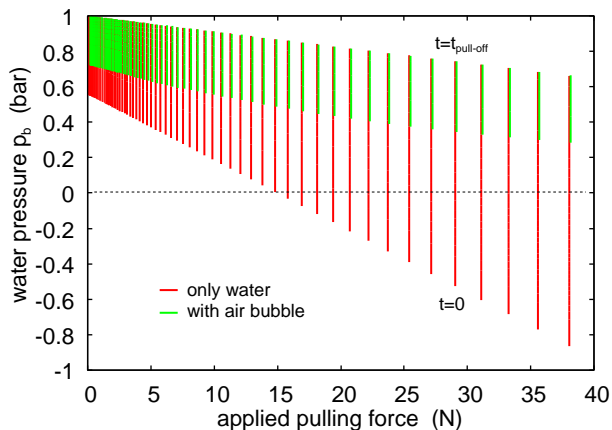


FIG. 14: The pressure  $p_b$  in the water inside the suction cup as a function of the applied pulling force. The vertical lines give the water pressure as the time changes from start of pull-off ( $t = 0$ ) to detachment ( $t = t_{\text{pull-off}}$ ). The red lines assumes only water inside the suction cup while the green lines assumes a small air bubble trapped in the initial state. In the latter case the water (and air) pressure inside the suction cup is always above the vacuum pressure  $p = 0$ , while in the first case, when the pull-off force is bigger than  $\approx 15$  N, the water pressure is negative for some initial time period.

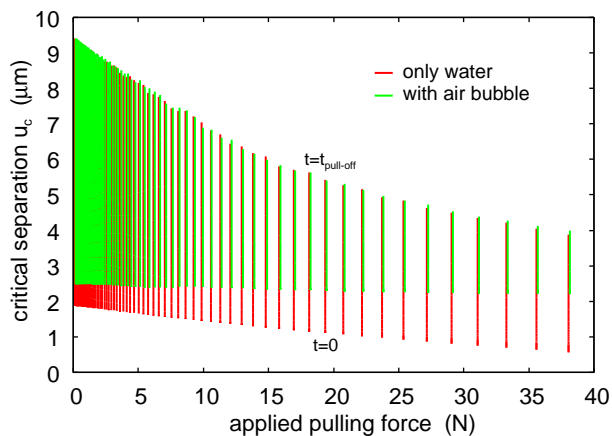


FIG. 15: The separation at the critical junction,  $u_c$ , as a function of the applied pulling force. The vertical lines give the critical separation as the time changes from start of pull-off ( $t = 0$ ) to detachment ( $t = t_{\text{pull-off}}$ ). The red lines assumes only water inside the suction cup, while the green lines assumes a small air bubble trapped in the initial state. The critical separation for short contact times is smaller in the former case owing to the lower fluid pressure in the suction cup, which pull the surfaces in the nominal contact strip  $l(t)$  closer together (see last term in (4)).

suction cup the pressure is always positive, but below the atmospheric pressure.

In the present experiments we have used distilled but not degassed water. We observed that even if no air bubbles can be detected inside the suction cup when immersed in the water, after squeezing it in contact with

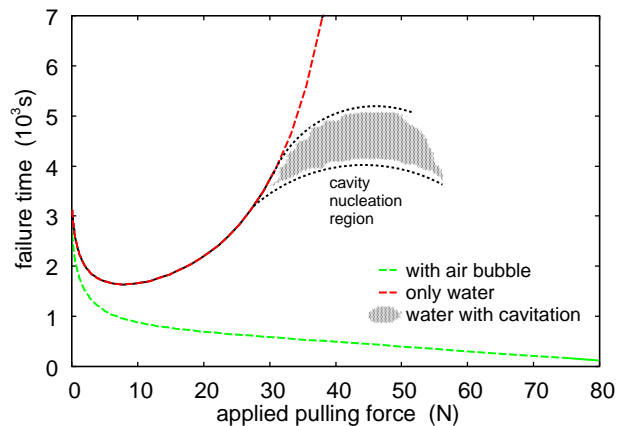


FIG. 16: A schematic picture illustrating the influence of cavitation on the failure time. For small applied pulling force the pressure in the water in the suction cup is not low enough to induce cavitation, but for large enough pulling-force cavitation occur. In this case, since cavitation is a stochastic process involving thermally activated nucleation of an air bubble, when the experiment is repeated many times large fluctuations in the failure time may occur (dotted region).

the counter surface and removing the applied squeezing force, we always observed a cavity region (gas bubble) at the top of the suction cup. That is, for water with dissolved air cavitation always occurred inside the suction cup due to the reduced pressure resulting from the spring force. We observed this even for a smooth glass substrate where no trapped micro or nano bubbles of gas is expected before application of the suction cup. (For the sandblasted PMMA, gas (air) may be trapped in roughness cavities.) Consequently, some air is always trapped inside the suction cup before application of the pull-off force  $F_1$ . Thus, the experimental results should be compared to the green line which assumes trapped air. The deviation between theory and experiments, observed mainly for applied forces above 30 N, may be due to capillary forces.

Fig. 13 shows the dependency of the logarithm of the failure time (time to pull-off) on the applied (pulling) force in water (green squares, from Fig. 12) and in the air (blue squares). The green and blue solid lines are the theory predictions assuming that in the initial state, before applying the pull-off force, there is some air inside the suction cup. The black dashed line is a fit-line to the experimental data in water.

In the air the failure time decreased from  $\approx 10$  s for the pull-off  $F_1 = 1.4$  N to  $\approx 5$  s for  $F_1 = 10$  N. In water the failure time was typically  $\approx 100$  times longer (see Fig. 13). This is also predicted by the theory (solid lines in 13) and is mainly due to the change in the viscosity which amount to a factor of  $\approx 56$  ( $\eta \approx 1.0 \times 10^{-3}$  Pas for water and  $\approx 1.8 \times 10^{-5}$  Pas for air). The factor  $Q$ , which is due to the finite compressibility of air and to ballistic air flow, is close



to unity in the present case. Since the rubber-substrate contact time is longer in water, and since the relaxation modulus decreases with increasing time (see Ref. [25]), in water the surfaces approach each other more closely in the contact strip  $l(t)$  than in air, which also tend to increase the failure time in water as compared to in air.

To get a deeper understanding of the failure process, in Fig. 14 we show the pressure  $p_b$  in the water inside the suction cup as a function of the applied pulling force. The vertical lines give the water pressure as the time changes from start of pull-off ( $t = 0$ ) to detachment ( $t = t_{\text{pull-off}}$ ). The red lines assumes only water inside the suction cup, while the green lines assumes a small air bubble trapped in the initial state. In the latter case the water (and air) pressure inside the suction cup is always above the vacuum pressure  $p = 0$ , while in the first case, when the pull-off force is bigger than  $\approx 15$  N the water pressure becomes negative for some initial time period.

Fig. 15 shows the separation at the critical junction,  $u_c$ , as a function of the applied pulling force. The vertical lines give the critical separation as the time changes from start of pull-off ( $t = 0$ ) to detachment ( $t = t_{\text{pull-off}}$ ). Again the red lines assumes only water inside the suction cup, while the green lines assumes a small air bubble trapped in the initial state. The critical separation for short contact times is smaller in the former case owing to the lower fluid pressure in the suction cup, which pull the surfaces in the nominal contact strip  $l(t)$  closer together (see last term in (4)).

Fig. 16 shows a schematic picture illustrating the influence of cavitation on the failure time. For small applied pulling force the pressure in the water in the suction cup is not low enough to induce cavitation, but for large enough pulling-force cavitation occur. In this case, since cavitation is a stochastic process involving thermally activated nucleation of an air bubble, when the experiment is repeated many times large fluctuations in the failure time may occur (dotted region).

## 7 Discussion

Many animals have developed suction cups to adhere to different surfaces in water, e.g., the octopus[30–33] or northern clingfish[34]. Studies have shown that these animals can adhere to much rougher surfaces than man-made suction cups. This is due to the very low elastic modulus of the material covering the suction cup surfaces. Thus, while most man-made suction cups are made from rubber-like materials with a Young’s modulus of order a few MPa, the suction cups of the octopus and the northern clingfish are covered by very soft materials with an effective modulus of order 10 kPa.

When a block of a very soft material is squeezed against a counter surface in water it tends to trap islands of water which reduces the contact area and the friction[35–37]. For this reason the surfaces of the soft adhesive discs in the octopus and the northern clingfish have channels

which allow the water to get removed faster during the approach of the suction cup to the counter surface. However, due to the low elastic modulus of the suction cup material, the channels are “flattened-out” when the suction cup is in adhesive contact with the counter surface, and negligible fluid leakage is expected to result from these surface structures.

There are two ways to attach a suction cup to a counter surface. Either a squeezing force is applied, or a pump must be used to lower the fluid (gas or liquid) pressure inside the suction cup. The latter is used in some engineering applications. However, it is not always easy for the octopus to apply a large normal force when attaching a suction cup to a counter surface, in particular before any arm is attached, and when the animal cannot wind the arm around the counter surface as may be the case in some accounts with sperm whale. Similarly, the northern clingfish cannot apply a large normal force to squeeze the adhesive disk in contact with a counter surface. So how can they attach the suction cups? We believe it may be due to changes in the suction cup volume involving muscle contraction as discussed in Ref. [25].

For adhesion to very rough surfaces, the part of the suction cup in contact with the substrate must be made from an elastically very soft material. However, using a very soft material everywhere result in a very small suction cup stiffness. We have shown (see in Ref. [25]) that a long lifetime require a large enough suction cup stiffness. Only in this case will the contact pressure  $p$  be large enough to reduce the water leak-rate to small enough values. Based on this, we have proposed a biomimetic design of an artificial suction cup having a elastically stiff membrane covered with a soft layer with a potential to stick to very rough surfaces under water, see ref. [25] for more details.

Recently two groups [19, 20], working on manufacturing of suction cups inspired from Northern clingfish, were successful in attaining high pull-off forces for rough surfaces in water. These devices utilize a relatively stiff material for the suction cup chamber, and a soft layer at the disc rim (with and without hierarchical structures), which increases the contact area with rough surfaces, and reduce the leakage of the fluid into the suction cups. Sandoval et. al.[20] also varied the design of suction cups, which included radial slits to remove water from the contact. It was suggested[19] that the use soft layer increases the friction on a rough substrate, and that this helps in reducing leakage. However, we believe that friction in itself is not very important, but the elastically soft layer reduces the surface separation and the leakage across the interface.

For suction cups used in the air the lowest possible pressure inside the suction cup is  $p_b = 0$ , corresponding to perfect vacuum. In reality it is usually much larger,  $p_b \approx 30 - 90$  kPa. For suction cups in water the pressure inside the suction cup could be negative where the

liquid is under mechanical tension. This state is only metastable, and negative pressures have been observed for short times[29]. For water in equilibrium with the normal atmosphere one expect cavitation to occur for any pressure below the atmospheric pressure, but the nucleation of cavities may take long time, and depends strongly on impurities and imperfections. For example, crack-like surface defects in hydrophobic materials may trap small (micrometer or nanometer) air bubbles which could expand to macroscopic size when the pressure is reduced below the atmospheric pressure.

Negative pressures have been observed inside the suction cups of octopus. Thus, in one study[38] it was found that most suction cups have pressures above zero, but some suction cups showed pressures as low as  $\approx -650$  kPa. We find this observation remarkable because for the suction cups we studied cavitation is always observed and the water pressure is therefore always positive.

Trapped air bubbles could influence the water flow into the suction cup by blocking flow channels. For not degassed water, whenever the fluid pressure falls below the atmospheric pressure cavitation can occur, and gas bubbles could form in the flow channels and block the fluid flow due to the Laplace pressure effect. For the suction cups studied above, in the initial state the Laplace pressure is likely to be smaller than the fluid pressure difference between inside and outside the suction cup, in which case the gas bubbles would get removed, but at a later stage in the detachment process this may no longer be true. This is similar to observations in earlier model studies of the water leakage of rubber seals, where strongly reduced leakage rates was observed for hydrophobic surfaces when the water pressure difference between inside and outside the seal become small enough[18].

## 8 Summary and conclusion

We have studied the leakage of suction cups both in air and water. The experimental results were analyzed using a newly developed theory of fluid leakage valid in diffusive and ballistic limits combined with Persson contact mechanics theory. In these experiments the suction cups (made of soft PVC) were pressed against sandblasted PMMA sheets. We found that the measured failure times of suction cups in air to be in good agreement with the theory, except for surfaces with rms-roughness below  $\approx 1 \mu\text{m}$ , where diffusion of plasticizer occurred, from the PVC to the PMMA counterface resulting in blocking of critical constrictions. For experiments in water, we found that the failure times of suction cup were  $\approx 100$  times longer than in air, and this could be attributed mainly to the different viscosity of air and water.

---

[1] B.N.J. Persson, *Sliding Friction: Physical Principles and Applications*, Springer, Heidelberg (2000).

- [2] E. Gnecco and E. Meyer, *Elements of Friction Theory and Nanotribology*, Cambridge University Press (2015).
- [3] J.N. Israelachvili, *Intermolecular and Surface Forces*, (Academic, London), 3rd Ed. (2011).
- [4] J.R. Barber, *Contact Mechanics (Solid Mechanics and Its Applications)*, Springer (2018).
- [5] B.N.J. Persson, *Contact mechanics for randomly rough surfaces*, Surface Science Reports **61**, 201 (2006).
- [6] B.N.J. Persson, O. Albohr, U. Tartaglino, A.I. Volokitin and E. Tosatti, *On the nature of surface roughness with application to contact mechanics, sealing, rubber friction and adhesion*, J. Phys.: Condens. Matter **17**, R1 (2005)
- [7] C. Creton, M. Ciccotti *Fracture and adhesion of soft materials: a review* Reports on Progress in Physics **79**, 046601 (2016).
- [8] R Spolenak, S Gorb, H Gao, E Arzt, *Effects of contact shape on the scaling of biological attachments*, Proceedings of the Royal Society A: Mathematical, Physical and Engineering Sciences **461**, 305 (2005).
- [9] L. Pastewka, M.O. Robbins *Contact between rough surfaces and a criterion for macroscopic adhesion*, Proceedings of the National Academy of Sciences **111**, 3298 (2014).
- [10] Martin H Müser, Wolf B Dapp, Romain Bugnicourt, Philippe Sainsot, Nicolas Lesaffre, Ton A Lubrecht, Bo NJ Persson, Kathryn Harris, Alexander Bennett, Kyle Schulze, Sean Rohde, Peter Ifju, W Gregory Sawyer, Thomas Angelini, Hossein Ashtari Esfahani, Mahmoud Kadkhodaei, Saleh Akbarzadeh, Jiunn-Jong Wu, Georg Vorlauffer, Andras Vernes, Soheil Solhjoo, Antonis I Vakis, Robert L Jackson, Yang Xu, Jeffrey Streater, Amir Rostami, Daniele Dini, Simon Medina, Giuseppe Carbone, Francesco Bottiglione, Luciano Afferrante, Joseph Monti, Lars Pastewka, Mark O Robbins, James A Greenwood, *Meeting the contact-mechanics challenge*, Tribology Letters **65**, 118 (2017).
- [11] AI Vakis, VA Yastrebov, J Scheibert, C Minfray, L Nicola, D Dini, A Almqvist, M Paggi, S Lee, G Limbert, JF Molinari, G Anciaux, R Aghababaei, S Echeverri Restrepo, A Papangelo, A Cammarata, P Nicolini, C Putignano, G Carbone, M Ciavarella, S Stupkiewicz, J Lengiewicz, G Costagliola, F Bosia, R Guarino, NM Pugno, MH Müser, *Modeling and simulation in tribology across scales: An overview*, Tribology International (TRIBINT-D-17-01694 - Accepted Manuscript).
- [12] A. Tiwari, *Adhesion, Friction and Leakage in Contacts with Elastomers*, PhD thesis, Publisher: NTNU (2018).
- [13] BNJ Persson Theory of rubber friction and contact mechanics, The Journal of Chemical Physics **115**, 3840 (2001)
- [14] W.B. Dapp, A. Lücke, B.N.J. Persson, and M.H. Müser *Self-Affine Elastic Contacts: Percolation and Leakage* Phys. Rev. Lett. **108**, 244301 (2012).
- [15] B. Lorenz, B.N.J. Persson, *On the dependence of the leak rate of seals on the skewness of the surface height probability distribution* Europhysics Letters **90**, 38002 (2010).
- [16] B. Lorenz, B.N.J. Persson *Leak rate of seals: Effective-medium theory and comparison with experiment* The European Physical Journal E **31**, 159 (2010).
- [17] B.N.J. Persson, C. Yang, *Theory of the leak-rate of seals*, J. Phys.: Condens. Matter **20**, 315011 (2008).
- [18] A. Tiwari, L. Dorogin, M. Tahir, K.W. Stöckelhuber, G. Heinrich, N. Espallargas, B.N.J. Persson, *Rubber contact mechanics: adhesion, friction and leakage of seals*, Soft

- Matter **13**, 9103 (2017).
- [19] P. Ditsche, A. Summers, *Learning from Northern clingfish (Gobiesox maeandricus): bioinspired suction cups attach to rough surfaces* Philosophical Transactions of the Royal Society B, 374(1784), 20190204 Sandoval (2019).
- [20] J. A. Sandoval, S. Jadhav, H. Quan, D.D. Deheyn, M. T. Tolley, *Reversible adhesion to rough surfaces both in and out of water, inspired by the clingfish suction disc* Bioinspiration and biomimetics, 14(6), 066016 (2019).
- [21] H. Iwasaki, F. Lefevre, D. D. Damian, E. Iwase, S. Miyashita, *Autonomous and Reversible Adhesion Using Elastomeric Suction Cups for In-Vivo Medical Treatments* IEEE Robotics and Automation Letters, 5 (2), 2015-2022 (2020).
- [22] A.L. Ruina, *Slip instability and state variable friction laws*, J. Geophys. res. **88**, 10359 (1983).
- [23] J.R. Rice and A.L. Ruina, *Stability of steady frictional slipping*, J. Appl. Mech. **50**, 343 (1983).
- [24] M.H. Nacer, *Tangential Momentum Accomodation Coefficient in Microchannels with Different Surface Materials*, PhD thesis, Marseille (2012).
- [25] A. Tiwari and B.N.J. Persson, *Physics of suction cup*, Soft Matter, 15(46), 9482-9499 (2019)
- [26] A. Almqvist, C. Campan, N. Prodanov and B.N.J. Persson, *Interfacial separation between elastic solids with randomly rough surfaces: Comparison between theory and numerical techniques*, Journal of the Mechanics and Physics of Solids **59**, 2355 (2011).
- [27] L. Afferrante, F. Bottiglione, C. Putignano, B.N.J. Persson, G. Carbone, *Elastic contact mechanics of randomly rough surfaces: an assessment of advanced asperity models and Persson's theory*, Tribology Letters **66**, 75 (2018).
- [28] Jung Hwan Kim, Seong Hun Kim, Chang Hyung Lee, Jae-Woon Nah, and Airan Hahn *DEHP Migration Behavior from Excessively Plasticized PVC Sheets*, Bull. Korean Chem. Soc. **24**, 345 (2003).
- [29] E. Herbert, S. Balibar, F. Caupin, *Cavitation pressure in water*, Phys. Rev. E **74**, 041603 (2006).
- [30] A.M. Smith, *Negative pressure generated by octopus suckers: a study of the tensile strength of water in nature*, J. exp. Biol. **157**, 257 (1991).
- [31] F. Tramacere, E. Appel, B. Mazzolai, S.N. Gorb, *Hairy suckers: the surface microstructure and its possible functional significance in the Octopus vulgaris sucker* Beilstein journal of nanotechnology **5**, 561 (2014).
- [32] K.K. Green, A. Kovalev, E.I. Svensson, S.N. Gorb, *Male clasping ability, female polymorphism and sexual conflict: fine-scale elytral morphology as a sexually antagonistic adaptation in female diving beetles*, Journal of the Royal Society Interface **10**, 20130409 (2013).
- [33] V. Tinnemann, L. Hernandez, S.C.L. Fischer, E. Arzt, R. Bennewitz and R. Hensel, *Adhesion: In Situ Observation Reveals Local Detachment Mechanisms and Suction Effects in Micropatterned Adhesives* Adv. Funct. Mater. **14**, 1807713 (2019)
- [34] D.K. Wainwright, T. Kleinteich, A. Kleinteich, S.N. Gorb, A.P. Summers, *Stick tight: suction adhesion on irregular surfaces in the northern clingfish*, Biology letters **9**, 20130234 (2013).
- [35] B.N.J. Persson and F. Mugele, *Squeeze-out and wear: fundamental principles and applications*, Journal of Physics: Condensed Matter **16**, R295 (2004).
- [36] A.D. Roberts, *The Physics of Tire Friction: Theory and Experiment*, ed D F Hays and A L Browne(New York: Plenum) (1974)
- [37] A.D. Roberts, D. Tabor, *The extrusion of liquids between highly elastic solids*, Proc. R. Soc. A **325**, 323 (1971).
- [38] W.M. Kier, A.M. Smith, *The structure and adhesive mechanism of octopus suckers*, Integr. Comp. Biol. **42**, 1146 (2002).